



ELSEVIER

New reduced molybdenum tellurides $(\text{Rb,Cs})_{n-2}\text{Mo}_{3n}\text{Te}_{3n+2}$ ($n = 4, 5, 6, 8$) containing condensed Mo_{3n} clusters

C. Thomas*, S. Picard, R. Gautier, P. Gougeon, M. Potel

Université de Rennes I, Laboratoire de Chimie du Solide et Inorganique Moléculaire, UMR 6511, Av. du Général Leclerc, 35042 Rennes Cedex, France

Abstract

The syntheses, crystal growths and crystal structures of the $(\text{Rb,Cs})_{n-2}\text{Mo}_{3n}\text{Te}_{3n+2}$ ($n = 4, 5, 6, 8$) compounds are reported. They crystallize in the space group $R\bar{3}$ for even n and in $P6_3/m$ for odd n . The Mo-Mo distances within the different Mo_{3n} clusters observed in the tellurides and the analogous sulfides and selenides synthesized previously are compared. Single crystal resistivity measurements on $\text{Cs}_2\text{Mo}_{12}\text{Te}_{14}$ show a metallic behaviour in the 2–300 K temperature range. © 1997 Elsevier Science S.A.

Keywords: Condensed clusters; Tellurides; Molybdenum

1. Introduction

In the large field of the ternary reduced molybdenum chalcogenides based on octahedral Mo_6 or trans-face-sharing condensed octahedral Mo_{3n} ($n = 3, 4, 5, 6, 7, 8$ and 10) clusters, very few tellurides have been synthesized. For instance, the only examples known to date are the $\text{M}_x\text{Mo}_6\text{Te}_8$ ($\text{M} = \text{Fe}, \text{Co}, \text{Ni}$) compounds containing octahedral Mo_6 clusters [1,2] and the quasi-one-dimensional $\text{M}_2\text{Mo}_6\text{Te}_6$ ($\text{M} = \text{Alkali metals, Tl, In}$) compounds with infinite linear chains of trans-face-sharing Mo_6 clusters [3,4]. In particular, contrary to sulfides and selenides, no tellurides based on isolated condensed octahedral clusters have been reported up to now.

We present here the syntheses, crystal structures and physical properties of the $(\text{Rb,Cs})_{n-2}\text{Mo}_{3n}\text{Te}_{3n+2}$ ($n = 4, 5, 6, 8$) compounds which are isostructural with the analogous selenides or sulfides [5–7].

2. Experimental

2.1. Syntheses

The two members of the series, $(\text{Cs,Rb})_2\text{Mo}_{12}\text{Te}_{14}$ ($n = 4$) and $\text{Cs}_3\text{Mo}_{15}\text{Te}_{17}$, ($n = 5$), have been obtained as single phase powders from stoichiometric mixtures of $(\text{Rb,Cs})_2\text{Mo}_6\text{Te}_6$ and Mo_6Te_8 (or MoTe_2 and Mo) heated either in evacuated silica tubes at 1500 K ($n = 4$) or in sealed molybdenum crucibles in the 1600–1800 K temperature range for 24 h ($n = 5$). Attempts to prepare pure powders of $(\text{Rb,Cs})_{n-2}\text{Mo}_{3n}\text{Te}_{3n+2}$ with $n = 6$ and 8 were unsuccessful and led to mixtures of Mo_{18} and Mo_{24} cluster compounds. The $(\text{Rb,Cs})_2\text{Mo}_6\text{Te}_6$ compounds were prepared by cationic exchange between $\text{In}_2\text{Mo}_6\text{Te}_6$ and alkali metal chloride at 1000 K in silica tubes [4]. Above 1800 K, decomposition occurs leading to considerable alkali metal telluride and telluride leakage through the molybdenum crucible.

Single crystals were obtained by prolonged annealing in sealed silica tubes at 1500 K in a vertical furnace having a natural temperature gradient in the

* Corresponding author.

Table 1
Crystallographic data for $\text{Cs}_{n-2}\text{Mo}_{3n}\text{Te}_{3n+2}$

| | $\text{Cs}_2\text{Mo}_{12}\text{Te}_{14}$ | $\text{Cs}_4\text{Mo}_{18}\text{Te}_{20}$ | $\text{Cs}_6\text{Mo}_{24}\text{Te}_{26}$ | $\text{Cs}_3\text{Mo}_{15}\text{Te}_{17}$ |
|---|---|---|---|---|
| Space group | $R\cdot\bar{3}$ | $R\cdot\bar{3}$ | $R\cdot\bar{3}$ | $P6_3/m$ |
| Hexagonal lattice: | | | | |
| a_H (Å) | 10.251(1) | 10.196(1) | 10.180(2) | 10.194(1) |
| c_H (Å) | 25.442(3) | 39.32(1) | 53.130(2) | 21.622(1) |
| V_H (Å ³) | 2315.3(7) | 3540(2) | 4768(4) | 1946(1) |
| Z_H | 3 | 3 | 3 | 2 |
| Rhombohedral lattice | | | | |
| a_R (Å) | 10.326(2) | 14.368(1) | 18.659(2) | |
| α_R (°) | 59.44(2) | 41.466(5) | 31.660(5) | |
| Crystal dimension (mm) | $0.14 \times 0.06 \times 0.05$ | $0.22 \times 0.10 \times 0.08$ | $0.22 \times 0.10 \times 0.09$ | $0.11 \times 0.04 \times 0.04$ |
| μ linear (cm ⁻¹) | 199.1 | 196.8 | 195.6 | 198.3 |
| Absorption correction | DIFABS | DIFABS | DIFABS | none |
| Absmin | 0.908 | 0.7343 | 0.877 | |
| Absmax | 1.1053 | 1.0919 | 1.0887 | |
| Θ range | $\Theta \leq 35^\circ$ | $\Theta \leq 30^\circ$ | $\Theta \leq 35^\circ$ | $\Theta \leq 35^\circ$ |
| Measured reflections | 2453 | 2503 | 4989 | 6211 |
| Independent reflections with $I > 2\sigma(I)$ | 1525 | 1685 | 2414 | 967 |
| R_{int} (%) | 2.1 | 6.3 | 2.6 | 3.9 |
| R (%) | 3.1 | 6.0 | 4.8 | 4.6 |
| R_w (%) | 3.5 | 7.0 | 4.9 | 4.3 |
| G.O.F. | 1.568 | 1.004 | 1.807 | 1.004 |

following way: the pellets of the starting mixtures were wrapped in a molybdenum foil in order to minimize the attack of the silica tube by alkali metals, and a molybdenum wire on which the single crystal grown was placed above the pellets.

These compounds crystallize in the space group $R\cdot\bar{3}$ for even n and $P6_3/m$ for odd n . Their lattice parameters are reported in Table 1. For $\text{Rb}_2\text{Mo}_{12}\text{Te}_{14}$, the crystals were systematically twinned with the following unit cell parameters in the hexagonal setting: $a = 10.158(1)$ Å and $c = 25.55(1)$ Å.

2.2. Structural studies

The intensity data of the different single crystals were collected on a CAD4 ENRAF-NONIUS diffractometer equipped with a graphite-monochromatized MoK α radiation ($\lambda = 0.71073$ Å) by $\theta-2\phi$ scan method. The atomic coordinates of the selenium analogous compounds were taken as initial values and full-matrix least square refinements on F of the positional and anisotropic displacement parameters for all atoms led to the final R values reported in Table 1 along with the experimental and refinement conditions. Final positional and isotropic equivalent displacement parameters are listed in Table 2. All calculations were performed with the MolEN [8] package on a Digital MicroVax 3100.

3. Results

These structures are characterized by networks of $\text{Mo}_{3n}\text{Te}_{3n+2}$ ($n = 4, 5, 6$ or 8) cluster units resulting from successive trans-face-sharing condensations of Mo_nTe_n units (Fig. 1).

As shown in Fig. 2 and Fig. 3, the stacking of the cluster units is different in the two structural models:

- in the space group $R\cdot\bar{3}$, they delimit channels, running along the three rhombohedral axes with inter-unit voids filled up by two, four, or six alkali cations in nine or 10 Te environments. Among the latter, six Te atoms occupy the apices of a trigonal prism and the remaining ones cap three or four faces;
- in $P6_3/m$, on one hand, the cluster units form linear channels parallel to the c axis in which the Cs(1) ions, in 4e position, are coordinated to nine Te atoms at the apices of a tricapped trigonal prism. On the other hand, cavities are formed between the cluster units, where the Cs(2) ions, in 2c position, are surrounded by 11 Te atoms forming a trigonal prism, the five faces of which are capped. All Cs-Te distances fall in the range of 3.76–4.04 Å as usually observed.

In Table 3, we have compared the Mo-Mo distances within the different Mo_{3n} clusters observed in the sulfides, selenides and tellurides. One can notice

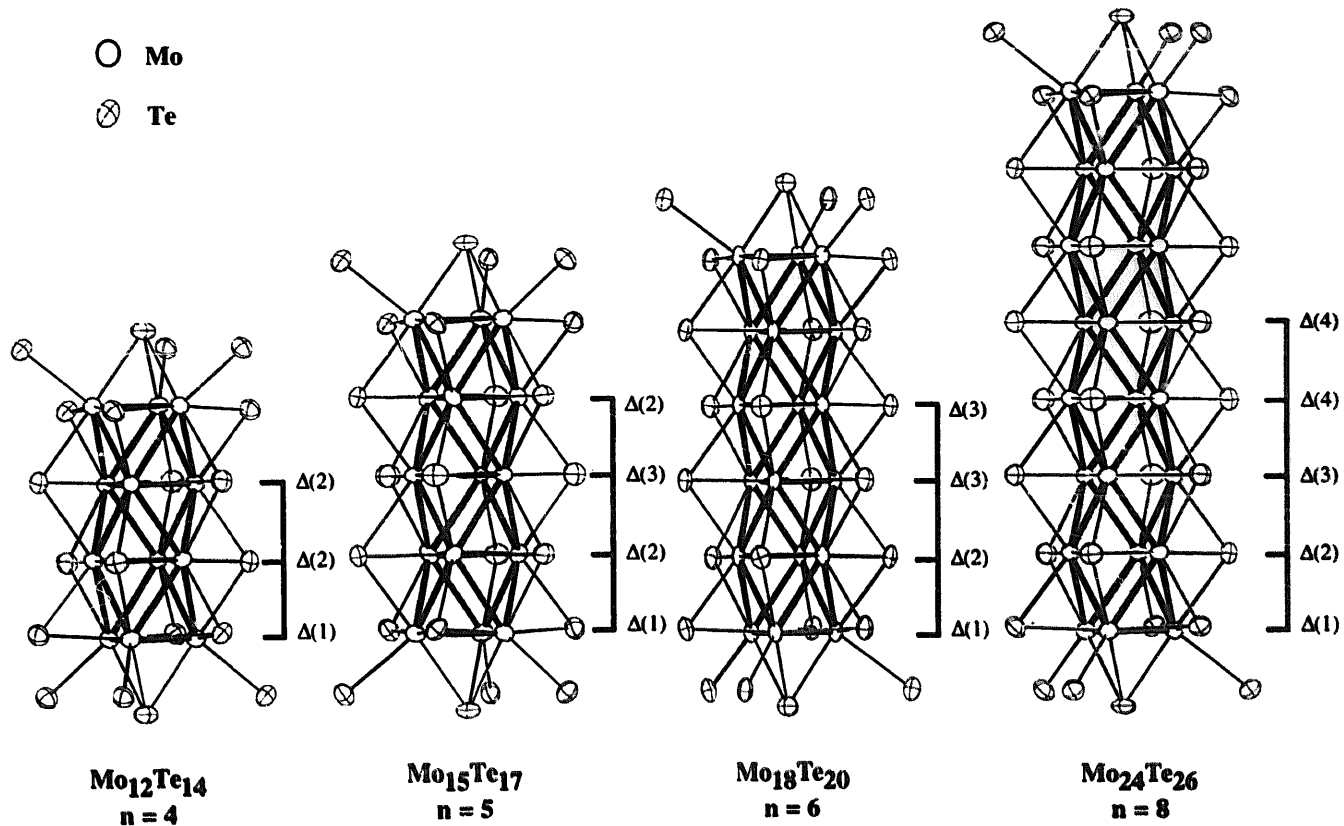
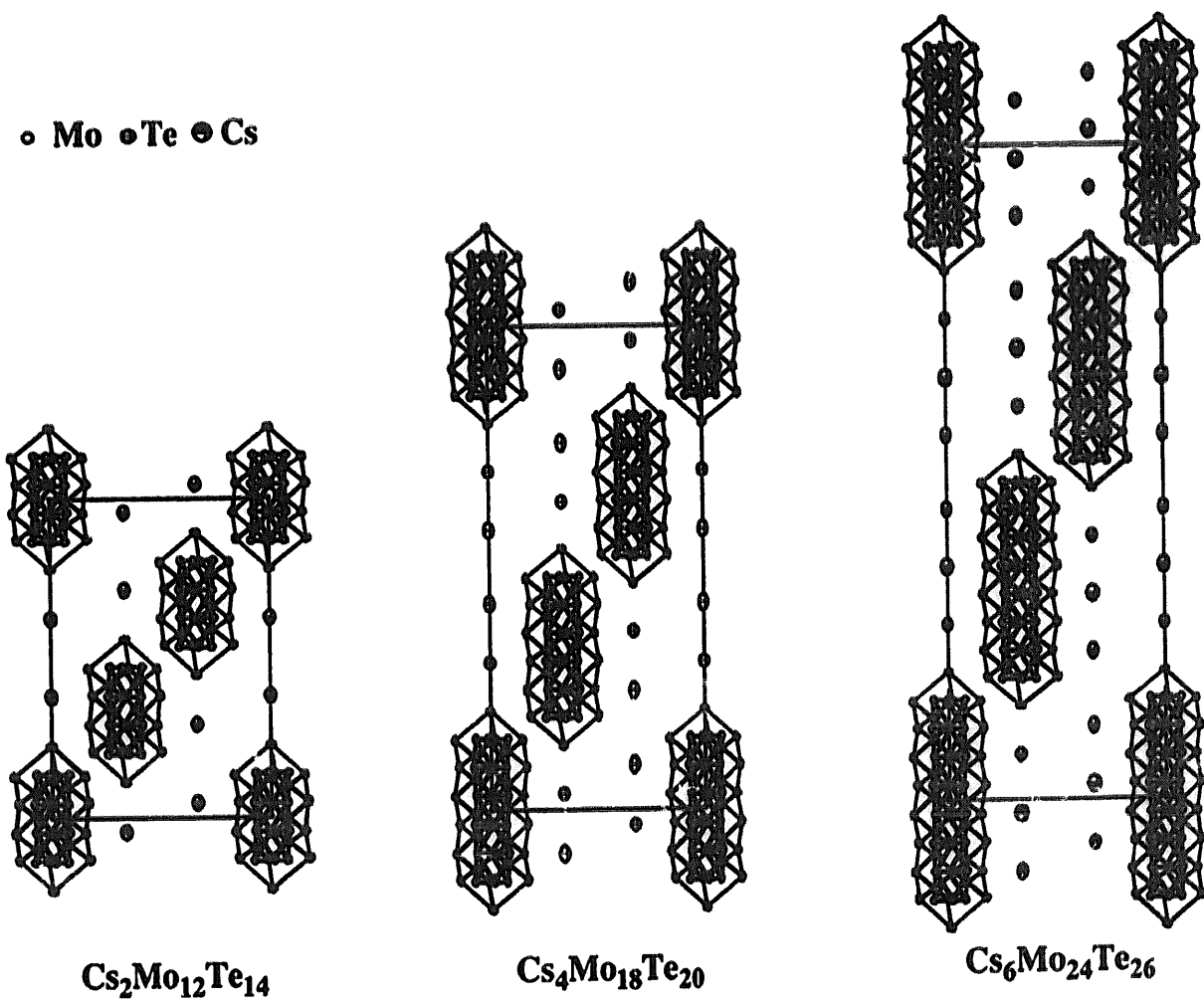
Fig. 1. $\text{Mo}_{30}\text{Te}_{3n+2}$ cluster units.

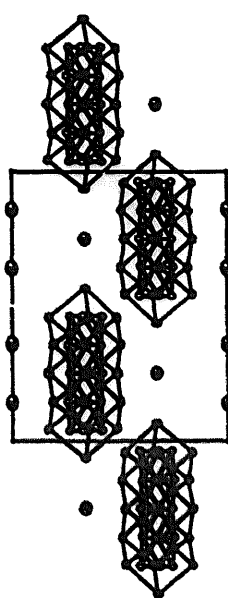
Fig. 2. Projections of the crystal structures of the even-membered compounds on the hexagonal (11-20) plane.

Table 2
Positional and equivalent isotropic displacement parameters for
 $\text{Cs}_{n-2}\text{Mo}_{3n}\text{Te}_{3n+2}$

| Atom | Position | x | y | z | B _{eq} (\AA^2) |
|---|----------|------------|------------|------------|------------------------------------|
| $\text{Cs}_2\text{Mo}_{12}\text{Te}_{14}$ | | | | | |
| Mo1 | 6f | 0.15786(7) | 0.13907(7) | 0.13588(2) | 0.60(1) |
| Mo2 | 6f | 0.01325(7) | 0.15756(7) | 0.04418(2) | 0.56(1) |
| Te1 | 6f | 0.37067(5) | 0.37059(5) | 0.20312(2) | 0.795(9) |
| Te2 | 6f | 0.32772(5) | 0.29686(6) | 0.04697(2) | 0.810(9) |
| Te3 | 2e | 0.0 | 0.0 | 0.22395(3) | 0.88(1) |
| Cs1 | 2e | 0.0 | 0.0 | 0.37766(5) | 1.93(1) |
| $\text{Cs}_3\text{Mo}_{15}\text{Te}_{17}$ | | | | | |
| Mo1 | 12i | 0.8264(2) | 0.4732(2) | 0.0375(1) | 0.56(4) |
| Mo2 | 12i | 0.8104(2) | 0.3180(2) | 0.1436(1) | 0.52(3) |
| Mo3 | 6h | 0.8250(3) | 0.4744(4) | 0.25 | 0.54(5) |
| Te1 | 6h | 0.3320(2) | 0.0367(2) | 0.04306(8) | 0.68(3) |
| Te2 | 12i | 0.3705(2) | 0.3681(2) | 0.14303(8) | 0.71(3) |
| Te3 | 12i | 0.3302(3) | 0.0367(3) | 0.25 | 0.91(5) |
| Te4 | 4f | 0.3333 | 0.6667 | 0.4336(1) | 0.71(3) |
| Cs1 | 4e | 0.0 | 0.0 | 0.1406(2) | 1.77(5) |
| Cs2 | 2e | 0.3333 | 0.6667 | 0.25 | 1.65(7) |
| $\text{Cs}_4\text{Mo}_{18}\text{Te}_{20}$ | | | | | |
| Mo1 | 6f | 0.1585(2) | 0.0186(2) | 0.14611(4) | 0.50(2) |
| Mo2 | 6f | 0.1438(1) | 0.1590(1) | 0.08730(4) | 0.47(2) |
| Mo3 | 6f | 0.1586(1) | 0.0180(1) | 0.02964(4) | 0.43(2) |
| Te1 | 6f | 0.2964(1) | 0.3342(1) | 0.14306(3) | 0.67(2) |
| Te2 | 6f | 0.3302(1) | 0.0342(1) | 0.08838(3) | 0.70(2) |
| Te3 | 6f | 0.2959(1) | 0.3366(1) | 0.02868(3) | 0.73(2) |
| Te4 | 2e | 0.0 | 0.0 | 0.20292(5) | 0.76(2) |
| Cs1 | 2e | 0.0 | 0.0 | 0.30133(6) | 1.58(3) |
| Cs2 | 2e | 0.0 | 0.0 | 0.42365(8) | 2.10(4) |
| $\text{Cs}_6\text{Mo}_{24}\text{Te}_{36}$ | | | | | |
| Mo1 | 6f | 0.1589(1) | 0.0192(1) | 0.15129(2) | 0.61(2) |
| Mo2 | 6f | 0.1442(1) | 0.1598(1) | 0.10794(2) | 0.55(2) |
| Mo3 | 6f | 0.1593(1) | 0.0190(1) | 0.06500(2) | 0.57(2) |
| Mo4 | 6f | 0.1399(1) | 0.1601(1) | 0.02134(2) | 0.55(2) |
| Te1 | 6f | 0.29693(9) | 0.33523(9) | 0.14906(2) | 0.79(1) |
| Te2 | 6f | 0.33136(9) | 0.03543(9) | 0.10851(2) | 0.76(1) |
| Te3 | 6f | 0.2958(1) | 0.33782(9) | 0.06452(2) | 0.84(2) |
| Te4 | 6f | 0.33819(9) | 0.0437(1) | 0.02193(2) | 0.90(2) |
| Te5 | 2e | 0.0 | 0.0 | 0.19344(3) | 0.79(2) |
| Cs1 | 2e | 0.0 | 0.0 | 0.26632(4) | 1.62(2) |
| Cs2 | 2e | 0.0 | 0.0 | 0.35500(5) | 2.72(3) |
| Cs3 | 2e | 0.0 | 0.0 | 0.44311(4) | 1.98(3) |

the homogeneity of the intra-triangle distances and the increase of the inter-triangle and inter-cluster distances when going from sulfides to selenides and tellurides. The inter-cluster distance increase is due to the steric effect of the chalcogenides while the inter-triangle distance increase is mainly due to an electronic effect, resulting from the increasing covalent character of the metal-ligand bonding from S to Se and Te atoms. This leads to a more important contribution of the chalcogen p orbitals to the conduction band and therefore to a decrease of the

• Mo • Te • Cs



$\text{Cs}_3\text{Mo}_{15}\text{Te}_{17}$

Fig. 3. Projection of the crystal structure of the odd-membered compound, $\text{Cs}_3\text{Mo}_{15}\text{Te}_{17}$, on the hexagonal (11-20) plane.

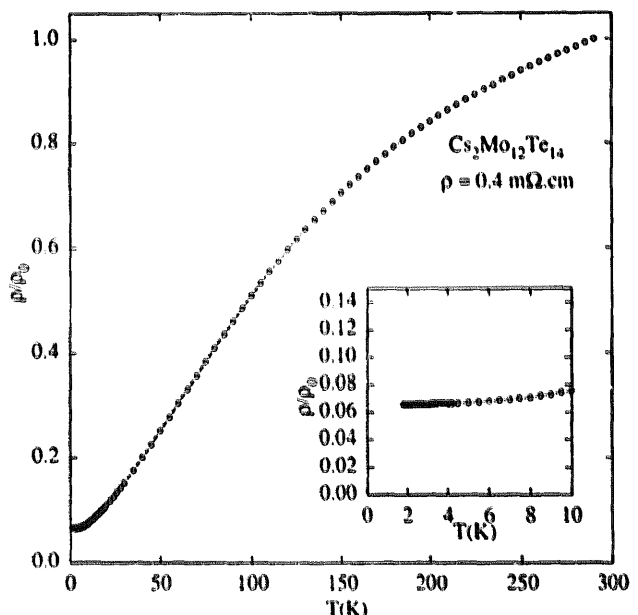


Fig. 4. Temperature variation of the normalized electrical resistivity of $\text{Cs}_2\text{Mo}_{12}\text{Te}_{14}$.

electronic density on the Mo clusters, reflected by the slightly larger Mo-Mo distances.

3.1. Resistivity measurements

Electrical resistivity measurements were carried out on a $\text{Cs}_2\text{Mo}_{12}\text{Te}_{14}$ (Fig. 4) single crystal in a standard four probe configuration over the 2–300 K tempera-

Table 3
Selected Mo-Mo distances for $\text{Cs}_{n-2}\text{Mo}_{3n}\text{Te}_{3n+2}$ compounds

| | | Intra-triangle Mo-Mo distances (\AA) | Inter-triangle Mo-Mo distances (\AA) | Inter-cluster Mo-Mo distances (\AA) | Inter-plane distances (\AA) | |
|---|---------|---|---|--|--|-----------------------|
| $\text{Cs}_2\text{Mo}_{12}\text{Se}_{14}$ | Mo1-Mo1 | 2.656(1) | Mo1-Mo2 | 2.758(1) 2.796(1) | 3.317(1) | $\Delta(1)-\Delta(2)$ |
| | Mo2-Mo2 | 2.682(1) | Mo2-Mo2 | 2.682(1) | | $\Delta(2)-\Delta(2)$ |
| $\text{Cs}_2\text{Mo}_{12}\text{Te}_{14}$ | Mo1-Mo1 | 2.651(1) | Mo1-Mo2 | 2.771(1) 2.820(1) | 3.700(2) | $\Delta(1)-\Delta(2)$ |
| | Mo2-Mo2 | 2.688(1) | Mo2-Mo2 | 2.733(1) | | $\Delta(2)-\Delta(2)$ |
| $\text{Cs}_3\text{Mo}_{15}\text{Se}_{17}$ | Mo1-Mo1 | 2.658(2) | Mo1-Mo2 | 2.737(1) | 3.310(2) | $\Delta(1)-\Delta(2)$ |
| | Mo2-Mo2 | 2.670(1) | Mo2-Mo3 | 2.767(1) 2.707(1) | | $\Delta(2)-\Delta(3)$ |
| | Mo3-Mo3 | 2.667(1) | Mo2-Mo3 | 2.722(1) | | 2.235(1) |
| $\text{Cs}_3\text{Mo}_{15}\text{Te}_{17}$ | Mo1-Mo1 | 2.666(4) | Mo1-Mo2 | 2.743(3) | 3.675(5) | $\Delta(1)-\Delta(2)$ |
| | Mo2-Mo2 | 2.684(6) | Mo2-Mo3 | 2.785(3) 2.760(3) | | $\Delta(2)-\Delta(3)$ |
| | Mo3-Mo3 | 2.654(6) | Mo2-Mo3 | 2.777(3) | | 2.301(1) |
| $\text{Cs}_4\text{Mo}_{18}\text{Se}_{20}^a$ | Mo1-Mo1 | 2.642(2) | Mo1-Mo2 | 2.740(1) | 3.343(2) | $\Delta(1)-\Delta(2)$ |
| | Mo2-Mo2 | 2.672(2) | Mo2-Mo3 | 2.770(1) 2.686(1) | | $\Delta(2)-\Delta(3)$ |
| | Mo3-Mo3 | 2.658(2) | Mo3-Mo3 | 2.735(2) | | 2.269(1) |
| $\text{Cs}_4\text{Mo}_{18}\text{Te}_{20}$ | Mo1-Mo1 | 2.651(2) | Mo1-Mo2 | 2.762(2) 2.794(2) | 3.696(3) | $\Delta(1)-\Delta(2)$ |
| | Mo2-Mo2 | 2.683(2) | Mo2-Mo3 | 2.728(2) 2.755(2) | | $\Delta(2)-\Delta(3)$ |
| | Mo3-Mo3 | 2.656(2) | Mo3-Mo3 | 2.789(2) | | 2.330(1) |
| $\text{Cs}_6\text{Mo}_{24}\text{S}_{26}$ [9] | Mo1-Mo1 | 2.649(1) | Mo1-Mo2 | 2.732(1) 2.746(1) | 3.181(2) | $\Delta(1)-\Delta(2)$ |
| | Mo2-Mo2 | 2.670(1) | Mo2-Mo3 | 2.663(1) 2.685(1) | | $\Delta(2)-\Delta(3)$ |
| | Mo3-Mo3 | 2.663(1) | Mo3-Mo4 | 2.702(1) 2.709(1) | | $\Delta(3)-\Delta(4)$ |
| | Mo4-Mo4 | 2.659(1) | Mo4-Mo4 | 2.693(1) | | 2.228(1) |
| $\text{Cs}_6\text{Mo}_{24}\text{Se}_{26}$ [9] | Mo1-Mo1 | 2.645(1) | Mo1-Mo2 | 2.736(1) 2.753(1) | 3.347(2) | $\Delta(1)-\Delta(2)$ |
| | Mo2-Mo2 | 2.673(2) | Mo2-Mo3 | 2.694(1) 2.716(1) | | $\Delta(2)-\Delta(3)$ |
| | Mo3-Mo3 | 2.656(2) | Mo3-Mo4 | 2.734(1) 2.743(1) | | $\Delta(3)-\Delta(4)$ |
| | Mo4-Mo4 | 2.660(2) | Mo4-Mo4 | 2.700(1) | | 2.218(1) |
| $\text{Cs}_6\text{Mo}_{24}\text{Te}_{26}$ | Mo1-Mo1 | 2.651(2) | Mo1-Mo2 | 2.756(2) 2.788(2) | 3.691(2) | $\Delta(1)-\Delta(2)$ |
| | Mo2-Mo2 | 2.691(2) | Mo2-Mo3 | 2.739(2) 2.770(2) | | $\Delta(2)-\Delta(3)$ |
| | Mo3-Mo3 | 2.655(2) | Mo3-Mo4 | 2.776(2) 2.786(2) | | $\Delta(3)-\Delta(4)$ |
| | Mo4-Mo4 | 2.662(2) | Mo4-Mo4 | 2.739(2) | | 2.268(1) |

^aPicard, unpublished results.

ture range. Ohmic contacts were made by attaching ultrasonically molten indium. The resistivity shows a linear decrease with the temperature and a smaller value ($\rho_{RT} = 0.4 \times 10^{-3} \Omega \text{ cm}^{-1}$, $\rho_{RT}/\rho_{5K} = 15$) than those previously observed for the selenium compounds ($\rho_{RT} = 6$ and $3 \times 10^{-3} \Omega \text{ cm}^{-1}$, $\rho_{RT}/\rho_{5K} = 4$

and 3 for $\text{Cs}_2\text{Mo}_{12}\text{Se}_{14}$ [5] and $\text{Rb}_2\text{Mo}_{12}\text{Se}_{14}$ (Picard, unpublished results), respectively) (Fig. 5). We think that this probably results from the increasing contribution of the p orbitals of the chalcogen at the Fermi level when going from selenium to tellurium.

Finally, contrary to the selenides which become

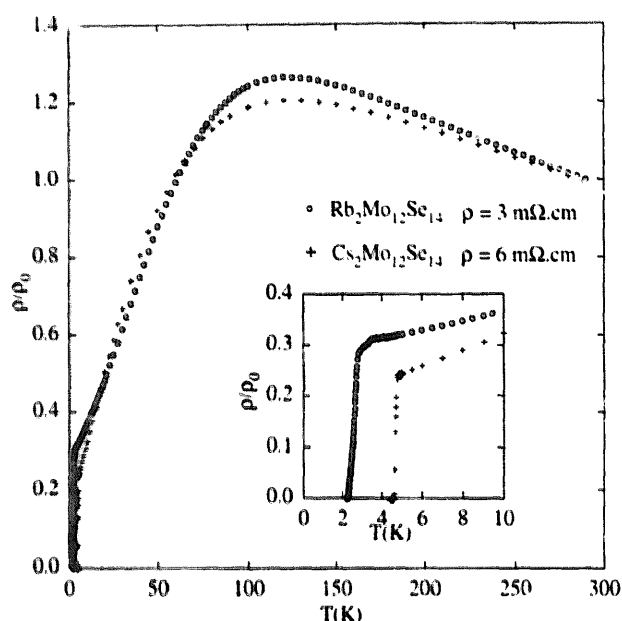


Fig. 5. Temperature variation of the normalized electrical resistivity of $\text{Cs}_2\text{Mo}_{12}\text{Se}_{14}$ and $\text{Rb}_2\text{Mo}_{12}\text{Se}_{14}$.

superconductors at 4.5 K and 2.5 K, respectively, no superconducting transition was observed down to 2 K for $\text{Cs}_2\text{Mo}_{12}\text{Te}_{14}$.

References

- [1] R. Chevrel, M. Sergent, in: Ø. Fischer, M.B. Maple (Eds.), Superconductivity in Ternary Compounds, vol. I, chapter 2, Springer, Berlin, 1982.
- [2] W. Höhle, K. Yvon, J. Solid State Chem. 70 (1987) 235.
- [3] M. Potel, R. Chevrel, M. Sergent, J.C. Armici, M. Decroux, Ø. Fischer, J. Solid State Chem. 35 (1980) 286–290.
- [4] M. Potel, P. Gougeon, R. Chevrel, M. Sergent, Rev. Chim. Minerale t71 (1984) 509–555.
- [5] P. Gougeon, M. Potel, J. Padiou, M. Sergent, Mater. Res. Bull. 22 (1987) 1087.
- [6] P. Gougeon, M. Potel, J. Padiou, M. Sergent, Mater. Res. Bull. 23 (1988) 453.
- [7] P. Gougeon, M. Potel, M. Sergent, Acta Cryst. C45 (1989) 1413.
- [8] C.K. Fair, MolEN. An interactive Intelligent System for Crystal Structure Analysis. Enraf-Nonius, Delft, The Netherlands, 1990.
- [9] P. Gougeon, Thesis, Rennes, France, 1984.